1

1   **Title:**

2   A preclinical randomized multicenter trial of anti-IL-17A treatment for acute ischemic stroke

3

4   **Authors:**

5   Mathias Gelderblom[1]*, Simon Koch[1], Jan-Kolja Strecker[2], Carina Jørgensen[3], Lidia Garcia-

6   Bonilla[4], Peter Ludewig[1], Christian Bernreuther[5], Hans Pinnschmidt[6], Thiruma V. Arumugam[7],

7   Goetz Thomalla[1], Cornelius Faber[8], Jan Sedlacik[9], Christian Gerloff[1], Jens Minnerup[2], Bettina H.

8   Clausen[3], Josef Anrather[4], Tim Magnus[1]

9

10   **Affiliations:**

11   [1] Department of Neurology, University Medical Center Hamburg-Eppendorf; Hamburg, Germany

12   [2] Department of Neurology with Institute of Translational Neurology, University of Münster;

13   Münster, Germany

14   [3] Department of Neurobiology Research, Institute of Molecular Medicine, University of Southern

15   Denmark; Odense, Denmark

16   [4] Feil Family Brain and Mind Research Institute, Weill Cornell Medicine, New York; New York,

17   USA

18   [5] Department of Neuropathology, University Medical Center Hamburg-Eppendorf; Hamburg,

19   Germany

20   [6] Institute of Medical Biometry and Epidemiology, University Medical Center Hamburg-

21   Eppendorf; Hamburg, Germany

22   [7] Department of Physiology, Anatomy & Microbiology School of Life Sciences, La Trobe

23   University; Melbourne, Australia

24   [8] Translational Research Imaging Center, Clinic of Radiology, University of Münster; Münster,

25   Germany

26   [9] Biomedical Engineering Department, Centre for the Developing Brain, School of Biomedical

27   Engineering & Imaging Sciences, King's College London; London, United Kingdom

28

29   **Corresponding Author:** Mathias Gelderblom, Department of Neurology, University Medical

30   Center Hamburg-Eppendorf, Martinistrasse 52, 20246 Hamburg, Germany,

31   m.gelderblom@uke.de, Tel.: ++49 152 2281 5359

32

33

34

35

36

37

38

39

40

41

42

Abstract

Multiple consensus statements have called for preclinical randomized controlled trials (pRCT) to improve translation in stroke research. Here, we investigated the efficacy of IL-17A neutralizing antibodies in a multicentric pRCT using a murine stroke model. C57/Bl.6 mice were subjected to transient middle cerebral artery occlusion (tMCAO). Mice were randomly allocated (1:1). Either anti-IL-17A (500 µg) or isotype antibody (500 µg) were administered 1 h after tMCAO. Primary analysis of infarct volumes was done by MRI after three days. Secondary analysis included mortality, neurological score, neutrophil infiltration and the impact of the gut microbiome on treatment effects. Out of 136 mice, 109 mice were included in the analysis. Mixed model analysis revealed that the IL-17A neutralization significantly reduced infarct sizes (anti IL-17A: 61.77 ± 31.04 mm^3; IgG control: 75.66 ± 34.79 mm^3; p=0.01). Secondary outcome measures showed a decrease in mortality (Hazard Ratio=3.43, 95% CI = 1.157 - 10.18; p=0.04) and neutrophil invasion into ischemic cortices. There was no difference in the neurological score. The analysis of the gut microbiome showed significant differences between centers. Taken together, this is the first positive pRCT in an ischemia reperfusion model. It suggests IL-17A neutralization as a potential target in stroke.

4

Introduction

66   The burden of stroke on society is substantial. Stroke is the leading cause of long term disability

67   in the Western World and an important reason for death worldwide (Collaborators, 2019).

68   Currently, therapy is limited to thrombolysis and thrombectomy, which is only available in

69   specialized centers. These facts clearly underline the need for novel therapeutic approaches.

70   However, it has been challenging to translate experimental findings from preclinical observations

71   to clinical application (Baker, 2016; O'Collins et al., 2006; Schmidt-Pogoda et al., 2020). These

72   translational difficulties have resulted in 2010 in the first ARRIVE guidelines and a recently

73   updated version ARRIVE 2.0 (Percie du Sert et al., 2020). A broad range of scientists have

74   supported and extended these guidelines with calls for rigorous study designs including

75   preclinical trials (Dirnagl et al., 2013; Landis et al., 2012). Conditions for multicenter preclinical

76   randomized controlled trials (pRCT) are: i) harmonized experimental protocol, ii) sample size

77   calculation, iii) randomization, iv) blinding, v) cross-validation, vi) centralized study

78   organization. With these prerequisites, such pRCTs are hard to organize and cost intensive.

79   Therefore, only one such trial exists in experimental stroke research (Llovera et al., 2015). Recent

80   immunological research has indicated that neuroinflammatory responses are promising

81   therapeutic targets in stroke (Chamorro, Dirnagl, Urra, & Planas, 2016). One of these targets is

82   the highly conserved pro-inflammatory cytokine Interleukin-17A (IL-17). IL-17A is implicated in

83   the pathology of several autoimmune diseases such as rheumatoid arthritis, and psoriasis, which

84   led to FDA approved anti-IL-17 treatments (Cua & Tato, 2010; Veldhoen, 2017). In experimental

85   stroke, evidence for a detrimental role of IL-17A was seen in multiple single-center studies

86   (Benakis et al., 2016; Dai et al., 2020; Gelderblom et al., 2012; Lee et al., 2020; Shichita et al.,

87   2009). While these data support an important role of IL-17A in stroke, single center studies are

88   biased by site-specific confounders, including animal housing conditions, the microbiome, the

89   experimental setup, and even the investigators.

90   Therefore, we have executed the first pRCT for IL-17A neutralization in experimental stroke.

91   This study was carried out in Odense (Denmark), New York (USA), Hamburg (Germany) and

92   Münster (Germany) using the temporal middle cerebral artery occlusion model (tMCAO).

93   Following a predefined, randomized, and blinded protocol, application of IL-17A antibodies

94   significantly reduced infarct size and mortality. Anti-IL-17A treatment resulted in less cortical

95   neutrophil infiltration. Sequencing the gut microbiome of mice from the different participating

96   laboratories revealed substantial differences of segmented filamentous bacteria (SFB), which are

97   potent inducers of IL-17A producing T cells. This pRCT showed that neuralization of IL-17A is

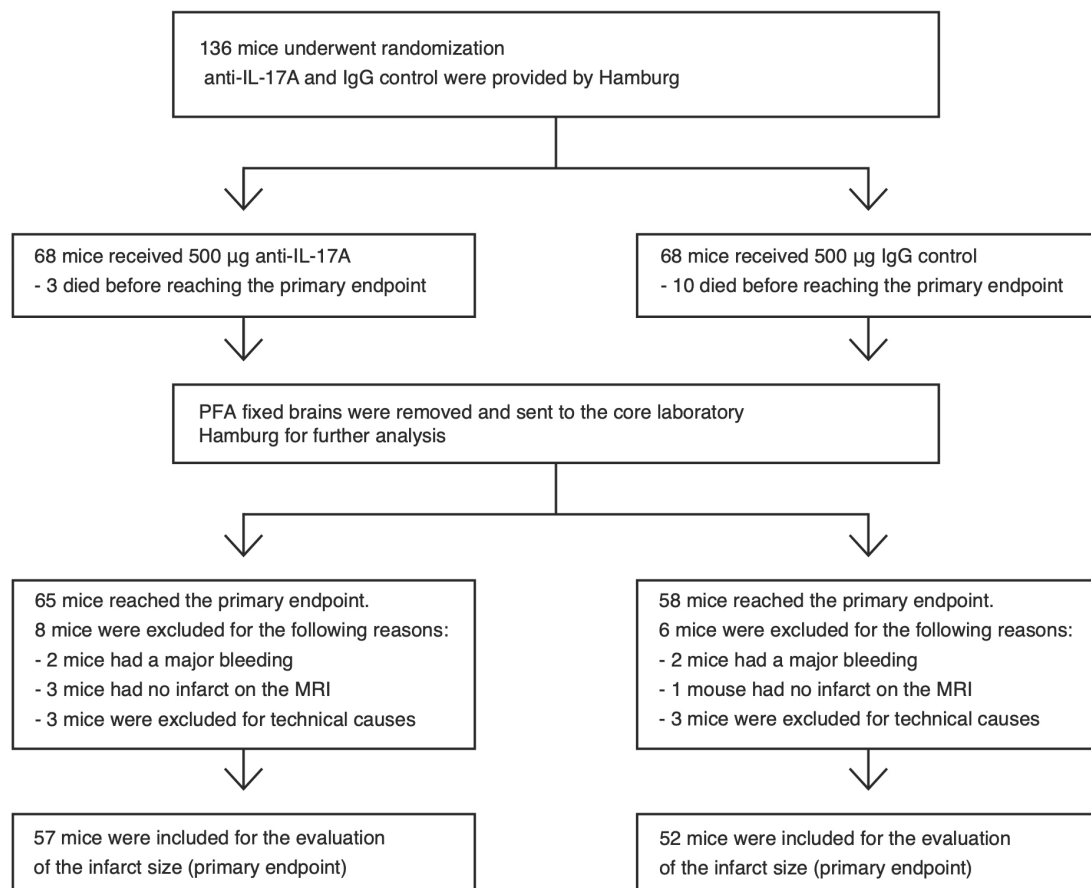98   effective in a large sample size and at different study centers.

99

Results

101   Study design:

102   A total of 136 C57Bl.6 mice were included in four independent research centers in Odense

103   (Denmark), New York (USA), Hamburg, and Münster (Germany) (Figure 1). tMCAO was

104   conducted for 45 minutes using the intraluminal filament method (6-0 nylon) (Gelderblom et al.,

105   2012). Coded antibodies (500 µg of anti-IL-17A (Clone MM17F3, eBioscience) or 500 µg of IgG

106   control) and filaments were provided by Hamburg. All of the participating surgeons and animal

107   caretakers were blinded for the treatment groups. The exclusion criteria were predefined in the

108   study protocol (Supplemental figure 1). Mice were allocated to the groups by the coordinating

109   center using a randomizer tool. All researchers were blinded with respect to the treatment groups.

110   Mice were randomized to treatment with either anti-IL-17A or isotype IgG antibody, which were

111   injected intravenously 1 h after occlusion. Primary endpoint was infarct size on day three in post-

112   mortal assessed MRI scans, secondary endpoints included mortality, and neurological scores.

113   Only mice with a reduction of the ipsilateral blood flow below 20% of the contralateral side as

114   measured by laser Doppler were included. Body temperature was controlled during surgery and

115   kept at 36°C. Three days following tMCAO, mice were sacrificed, brains were removed, and sent

116   to the core laboratory in Hamburg for evaluation of infarct size by two independent blinded

117   investigators. Unblinding was performed following completion of the statistical analyses. In the

118   anti-IL-17A group, eight mice were excluded for the following reasons: major intracerebral

119   bleeding (n=2), undetectable infarct on the MRI (n=3) or technical causes (n=3). In the isotype

120   IgG control group, six mice were excluded for the following reasons: major intracerebral

121   bleeding (n=2), undetectable infarct on the MRI (n=1) or technical causes (n=3). The mortality

122   until day 3 was n=3 in the IL-17A treatment group and n=10 in the isotype control group. A total

123   of 109 mice was included in the analysis of the primary endpoint (IL-17A treatment group n=57;

124   isotype control group n=52).

125

126

127

Figure 1

```
┌─────────────────────────────────────────────────────────────┐
│ 136 mice underwent randomization                             │
│  anti-IL-17A and IgG control were provided by Hamburg        │
└─────────────────────────────────────────────────────────────┘
```

```
┌──────────────────────────────────────┐   ┌──────────────────────────────────────┐
│ 68 mice received 500 µg anti-IL-17A   │   │ 68 mice received 500 µg IgG control   │
│ - 3 died before reaching the primary  │   │ - 10 died before reaching the primary │
│   endpoint                            │   │   endpoint                            │
└──────────────────────────────────────┘   └──────────────────────────────────────┘
```

```
┌─────────────────────────────────────────────────────────────┐
│ PFA fixed brains were removed and sent to the core laboratory │
│ Hamburg for further analysis                                  │
└─────────────────────────────────────────────────────────────┘
```

```
┌──────────────────────────────────────┐   ┌──────────────────────────────────────┐
│ 65 mice reached the primary endpoint. │   │ 58 mice reached the primary endpoint. │
│ 8 mice were excluded for the          │   │ 6 mice were excluded for the          │
│ following reasons:                    │   │ following reasons:                    │
│ - 2 mice had a major bleeding         │   │ - 2 mice had a major bleeding         │
│ - 3 mice had no infarct on the MRI    │   │ - 1 mouse had no infarct on the MRI   │
│ - 3 mice were excluded for technical  │   │ - 3 mice were excluded for technical  │
│   causes                              │   │   causes                              │
└──────────────────────────────────────┘   └──────────────────────────────────────┘
```

```
┌──────────────────────────────────────┐   ┌──────────────────────────────────────┐
│ 57 mice were included for the         │   │ 52 mice were included for the         │
│ evaluation of the infarct size        │   │ evaluation of the infarct size        │
│ (primary endpoint)                    │   │ (primary endpoint)                    │
└──────────────────────────────────────┘   └──────────────────────────────────────┘
```

128

129 **Figure 1. Design of the preclinical randomized multicenter study.**

130 Illustration of included and excluded animals. Mice were treated either with 500 µg of anti-IL-
131 17A or 500 µg of IgG control 1 h following reperfusion. Randomization of antibodies and
132 blinded analysis of infarct volumes were performed in the core laboratory in Hamburg. Only
133 brains of mice that survived until day three underwent final analysis of infarct volumes.
134

135

136 Neutralization of Interleukin-17A protects from ischemic stroke and reduces mortality:

137 Infarct sizes were determined in a blinded approach by the volume of the apparent diffusion

138 coefficient (ADC) lesion in post mortem brains as assessed by magnetic resonance imaging

139 (MRI) scans. Three days following tMCAO, the mean infarct volume and SD in the pooled data

140 set was 61.77 ± 31.04 mm^3 in the anti-IL-17A treatment group and 75.66 ± 34.79 mm^3 in the IgG

8

141   control group. To analyze the effects of the IL-17A neutralization, we employed a linear-mixed

142   model analysis with the two investigators as random effects, which revealed significantly reduced

143   infarct sizes in anti-IL-17A treatment group when compared to the IgG control group (Figure 2A,

144   B). Furthermore, mortality was significantly reduced in the anti-IL-17A group (Figure 2C, D).

145   The probability of mice of the IgG control group to die was more than three times higher than in

146   the anti-IL-17A group (Hazard Ratio=3.43, 95% CI = 1.157 - 10.18). Neurological scores

147   (Supplemental Figure 2A) and weight loss until day three (Supplemental Figure 2B) did not

148   differ between groups.

149

9
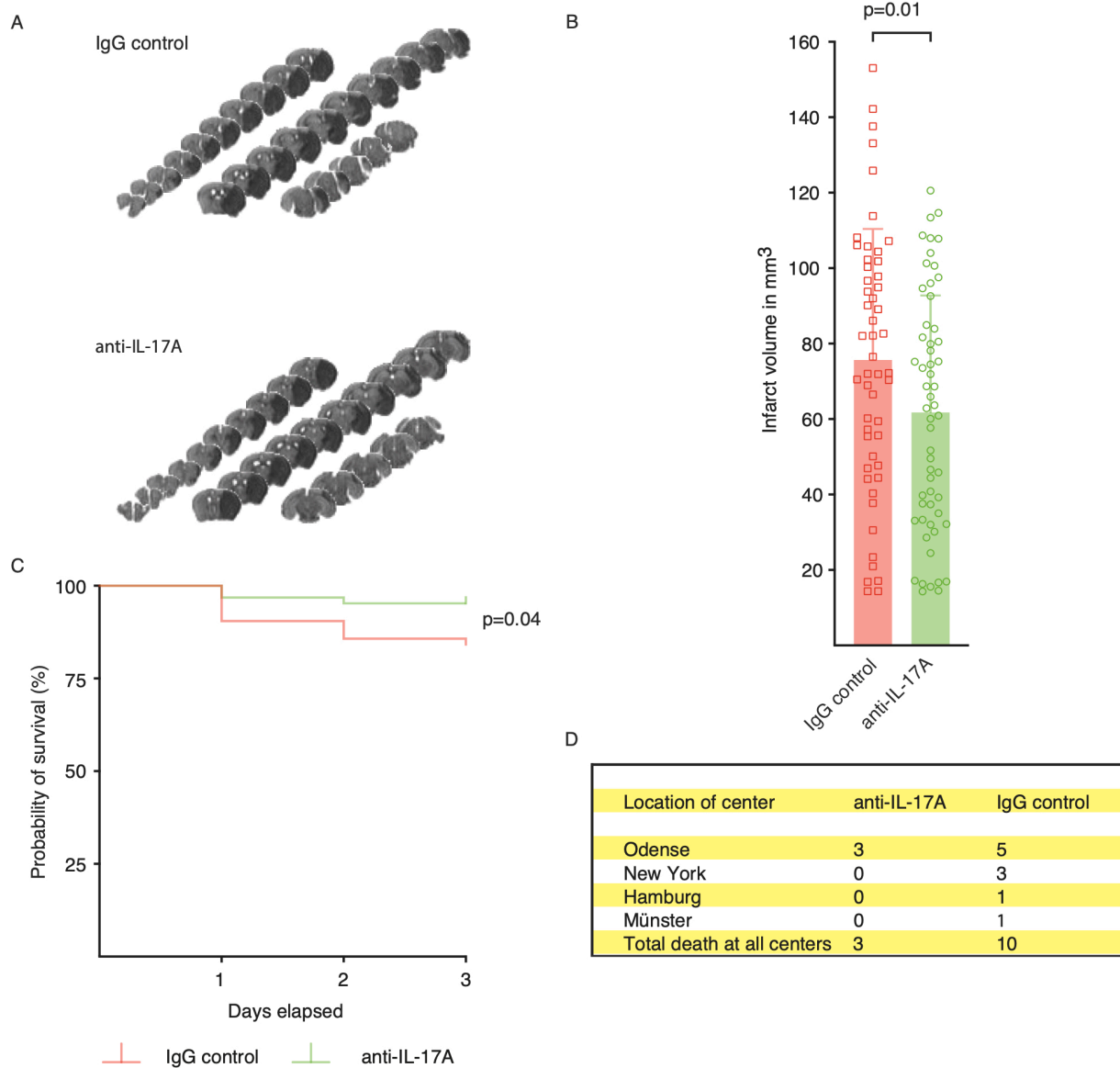
Figure 2

Figure 2. Neutralization of IL-17A significantly reduced infarct size and lowered mortality.

(A) Representative MRI images of ADC weighted images. (B) Pooled data from all test centers.
Infarct volumes were analyzed three days following tMCAO by MRI. The infarct volumes of
rater one are shown in mm^3. Graphs show mean±SDs. Statistical significance was assessed by
linear-mixed model analysis ($F_{(1,209)}$=6.56, p=0.01, n=109). (C, D) Survival rate and number of
dead mice. Statistical significance was assessed by a log-rank test ($\chi^2_{(1)}$=4.15, p=0.04, n=123).

159

160   IL-17A neutralization reduced lesion sizes of cortical infarcts:

161   Next, we analyzed the effects of the IL-17A neutralization on infarcts with or without

162   involvement of cortical regions. We distinguished between lesions that affected the cortex and

163   striatum and lesions that were limited to striatal areas and were therefore smaller on average. The

164   pooled data showed that the neutraxlization of IL-17A significantly reduced infarcts with cortical

165   involvement (Figure 3A). In contrast, an analysis of purely striatal infarcts showed no trend

166   towards smaller infarcts in the anti-IL-17A group (Figure 3B).

Figure 3

167

Figure 3. IL-17A neutralization reduced only cortical infarcts.

169   (A) Analysis of combined cortical and striatal infarct volumes (pooled data set). Infarct volumes
170   of rater one are shown in mm3. Graphs show mean±SDs. Statistical analysis was assessed by
171   linear-mixed model analysis ($F_{(1,185)}=8.91$, $p<0.01$, n=97). (B) Analysis of purely striatal infarct
172   volumes ($F_{(1,16)}=2.26$, $p=0.15$, n=12)).

173   The activation of the IL-17A axis can be tracked by the analysis of neutrophil

174   infiltration(Gelderblom et al., 2012). We assessed infiltrating neutrophils in different brain

175   regions on day three following tMCAO by flow cytometry. The analysis revealed a significant

176   relative (Figure 4A) and absolute (Figure 4B) increase of neutrophils in cortical areas compared

177   to striatal areas. We also investigated neutrophil numbers in postmortem brain tissue of mice

178   from our multicenter trial. Brains were sectioned, and absolute neutrophil numbers were

179   quantified following immunohistochemical Ly6G staining. Again, we found in the IgG control

180   group that neutrophils predominantly migrated into cortical areas. When we compared the anti-

181   IL17A with the IgG control group, we found a highly significant inhibitory effect of the anti-IL-

182   17A treatment on the neutrophil infiltration in the cortex but not the striatum (Figure 4C, D). In

183   order to demonstrate the translational relevance of our findings, we examined neuropathological

184   samples from a patient who had died 24 h after having a stroke. In this tissue, H&E staining

185   showed cells with unequivocal physical characteristics of neutrophils (polymorphonuclear) and

186   few monocytes in the edematous parenchyma (Figure 4E). In summary, we showed that the anti-

187   IL-17A treatment is predominantly effective in cortical infarcts and that it results in reduced

188   migration of neutrophils into cortical areas.

189

Figure 4

190
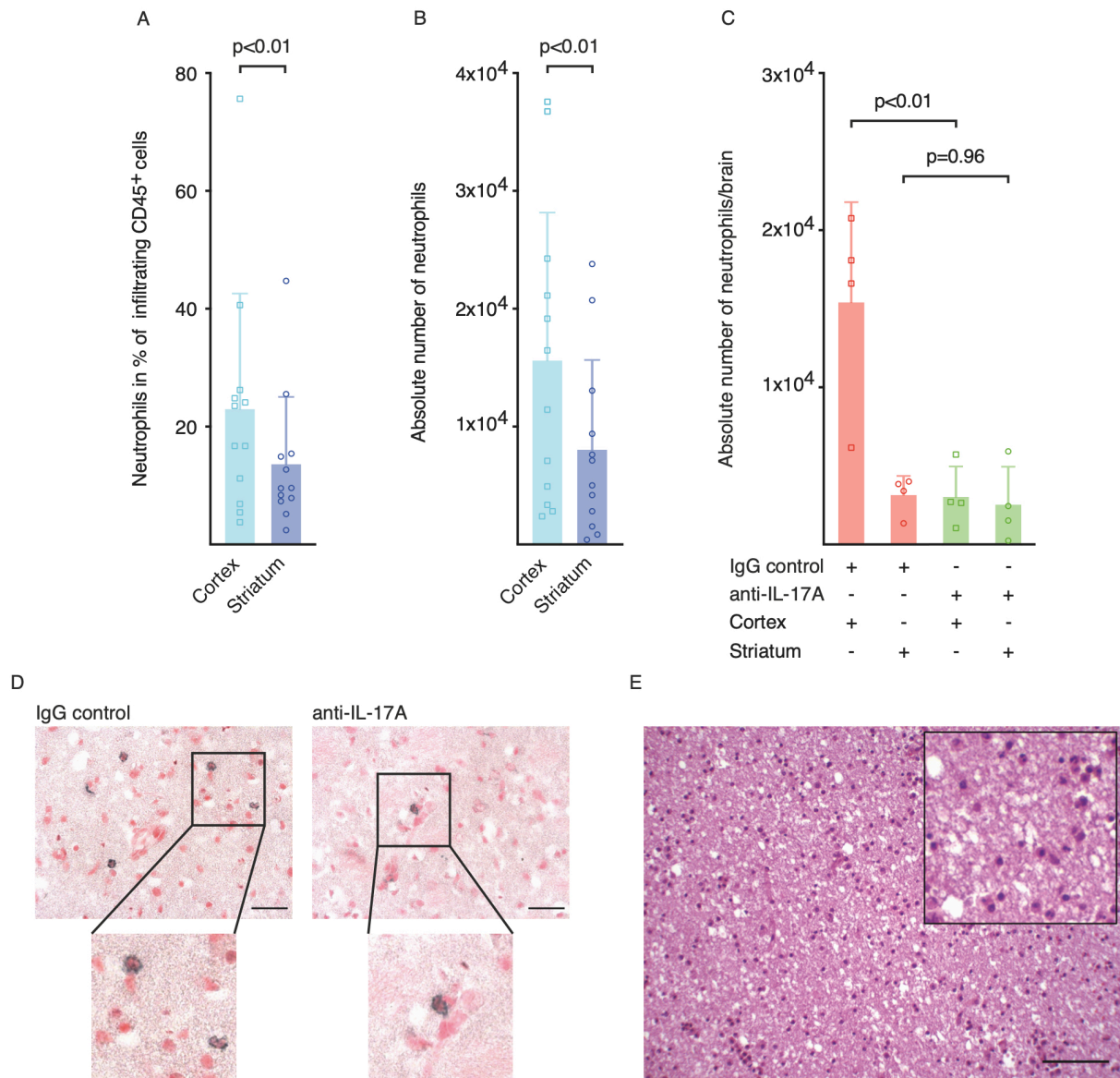
Figure 4. IL-17A neutralization diminished neutrophil infiltration into the cortex.

(A) Percentages of neutrophils in infiltrating $CD45^+$ cells and (B) absolute numbers of neutrophils in cortical and striatal brain tissue three days following tMCAO. Graphs show mean±SDs. (Students t-test for dependent variables, (A) $t_{(11)}=3.68$, $p<0.01$, n=12; (B) $t_{(11)}=3.8$, $p<0.01$, n=12). Cell counts were determined by flow cytometric analysis of CNS-infiltrating cells. (C) Quantitative analysis of $Ly6G^+$ cell counts per ipsilateral hemisphere in representative animals of our trial. Graphs show mean±SDs. Statistical analysis was performed with a two-factorial analysis of variances with repeated measures and Šidák's multiple comparison tests for pairwise comparisons (Cortex: $t_{(12)}=4.85$, $p<0.01$, Striatum: $t_{(12)}=0.24$, $p=0.965$, n=8)). (D) Immunohistochemical staining of neutrophils (Ly6G) in mice from both treatment groups 3 days

201 after tMCAO (scale bar 20 μm). (E) H&E staining of ischemic human brain tissue 24 hours after
202 stroke (scale bar 100 μm).

203

204 The gut microbiome differs in between the four centers:

205 The gut microbiome influences the immune response and the overall outcome following stroke

206 (Xia et al., 2019). In order to determine differences in the composition of the microbiome and

207 thus a possible influence on stroke outcome, we sequenced the variable regions v3 and v4 of the

208 16S rRNA of the gut bacteria. Specimens of 10 specific pathogen free (SPF) mice of each center

209 were collected. The analysis of the operational taxonomic units (OTUs), revealed significant

210 differences in the species diversity between most study centers (Figure 5A, B). Furthermore, the

211 principal coordinate analysis showed distinct clusters, clearly distinguishing the four test centers

212 (Figure 5C).

213 The single center analyzes of infarct sizes had revealed that one center (Odense) showed no effect

214 of the IL-17A treatment (Supplemental Figure 3A, B). The colonization with segmented

215 filamentous bacteria (SFB) can induce IL-17A producing T cells (Ivanov et al., 2009). SFB were

216 assessed by quantitative real-time PCR in the fecal material. The qPCR showed that animals from

217 Odense had significantly higher amounts of SFB compared to Münster and Hamburg, while in

218 New York no SFB were detectable (Figure 5D). In summary, the data showed that the

219 microbiome and the SFB levels significantly differed between the four test centers and that the

220 colonization with SFB correlated with a worse response to IL-17A neutralization.

221

Figure 5

222
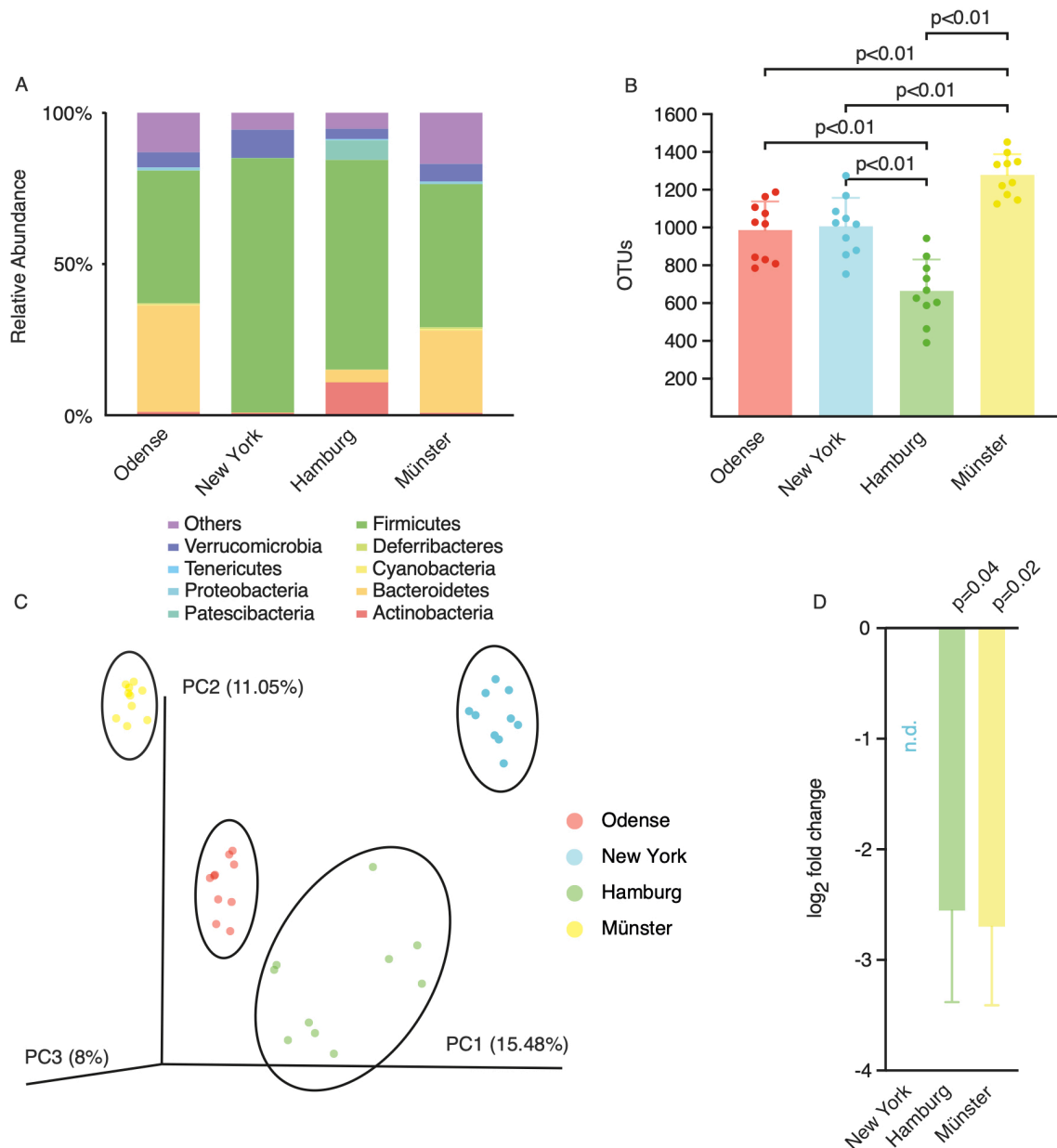
Figure 5. The microbiome differs between the four centers.

(A) Taxonomic summary of OTUs on phylum level, n=10 in each center. (B) Total numbers of OTUs for each center. Graphs show mean±SDs. Statistical significance was assessed by pairwise t-tests for independent samples (New York vs. Odense: t=0.29, p=1; New York vs. Hamburg, t=4.76, p=0.001; New York vs. Münster: t=-4.55, p=0.004; Hamburg vs. Odense: t=-4.48, p=0.002; Hamburg vs. Münster: t=-9.65, p<0.001; Münster vs. Odense: t=-4.88, p=0.001, n=10 in each center). (C) Principle coordinate analysis (PCoA) of the family composition. Clusters of each center are highlighted with an ellipse. Statistical testing was performed with an analysis of similarities (R=0.78, p<0.001, n=40). (D) qPCR analysis for SFB presence in mice from the four different centers. Expression levels were normalized to corresponding SFB levels in mice from

233 Odense. Shown is the log2 fold change as means±SDs. SFB were not detectable in the New York
234 cohort. Statistical significance was assessed by t-tests for independent samples (Hamburg:
235 $t_{(14)}$=2.23, p=0.04, n=16; Münster: $t_{(16)}$=2.58; p=0.02, n=18).

236

Discussion

238 This pRCT provides evidence that IL-17A neutralization results in smaller infarcts and improved

239 survival. These findings confirm the results from single center studies investigating the impact of

240 IL-17A on stroke outcome (Benakis et al., 2016; Gelderblom et al., 2012; Shichita et al., 2009).

241 Recent consensus statements have indicated the need for pRCTs to validate and eventually

242 translate experimental research. Our trial followed the given guidelines (Dirnagl et al., 2013) and

243 is the first positive pRCT in stroke using the tMCAO model.

244 There are several experimental stroke models available: the tMCAO, the permanent MCAO

245 (pMCAO), and the photothrombosis (ptMCAO) model (Sommer, 2017). tMCAO resembles the

246 occlusion/reperfusion injury of a proximal middle cerebral artery (MCA) infarct in humans while

247 pMCAO and ptMCAO are similar to distal cortical infarcts of the MCA. The advantage of

248 pMCAO and ptMCAO is a smaller variability in stroke size and, therefore, smaller effects can be

249 detected more easily (Lipsanen & Jolkkonen, 2011). Compared to the human situation, the

250 downsides of these two models are the artificial opening of the dura mater (pMCAO) or the use

251 of the radical inducing chemical rose Bengal (ptMCAO). tMCAO, as in our trial, has a much

252 higher variability including cortical and subcortical infarcts but corresponds better to the

253 variability seen in human trials (Elkins et al., 2017; Llovera et al., 2015; Lovblad et al., 1997).

254 This dilemma is also documented in the only other pRCT in experimental stroke research. In this

255 trial, Llovera and colleagues investigated the effects of CD49d-specific antibodies (Llovera et al.,

256 2015). A significant reduction of infarct volume was only documented for pMCAO but not for

257   tMCAO. Subsequent human trials (ACTION 1 and 2) using CD49d-specific antibodies failed to

258   find any effect on stroke progression (Elkind et al., 2020; Elkins et al., 2017). However, the range

259   in infarct volume with 1 - 212 ml in the clinical study compared better to the non-significant

260   tMCAO (0.001 - 0.095 ml) but not to the significant pMCAO results (0,003-0,016 ml) (Elkins et

261   al., 2017; Llovera et al., 2015). Consequently, two different approaches seem feasible. First, only

262   therapeutics, which result in significant beneficial effects despite a high variability in a pRCTs,

263   should enter human stroke trials. Second, should a therapeutic have a significant benefit in a

264   pRCT with low variability (e.g. pMCAO, ptMCAO), the corresponding human stroke trial should

265   use inclusion criteria ensuring low variability. In our anti-IL-17A trial, the range in stroke volume

266   was 0.0013 - 0.15 ml, which corresponds to the variability of stroke volumes in most human

267   studies (Elkins et al., 2017; Ganesan, Ng, Chong, Kirkham, & Connelly, 1999; Lovblad et al.,

268   1997).

269   The main physiological function of IL-17A is to induce innate immune responses towards

270   pathogens resulting in a rapid upregulation of neutrophil attracting chemokines (reviewed by

271   (McGeachy, Cua, & Gaffen, 2019; Veldhoen, 2017)). In our study, we could demonstrate that the

272   neutralization of IL-17A led to a diminished migration of neutrophils to the brain. Interestingly,

273   the overall infiltration of neutrophils and their inhibition by anti-IL-17A treatment was much

274   more prominent in ischemic cortical areas than subcortical/striatal areas. This finding could

275   explain why IL-17A neutralization was only effective in animals with cortical infarcts. A

276   potential reason for this tropism of neutrophils to cortical areas, is that IL-17A$^+$ γδ T cells are

277   mostly located in the meninges (Alves de Lima et al., 2020; Benakis et al., 2016; Ribeiro et al.,

278   2019).

279   However, IL-17A signaling in the brain does not only have detrimental effects. IL-17A from

280   meningeal γδ T cells can support short-term memory and synaptic plasticity through induction of

281   glial brain-derived-neurotrophic factor (BDNF) (Ribeiro et al., 2019). This dichotomy of IL-17A

282   effects in the CNS is likely explained by the micro milieu in affected target tissues. Net outcomes

283   of the IL-17 receptor activation strongly depend on the cellular target and the cooperative

284   stimulation by other cytokines. This cooperation results in synergistic activation of downstream

285   signaling pathways (Ruddy et al., 2004). In particular, IL-17A synergizes with strong NF-κB

286   activators, such as IL-1β and TNF-α, which are both rapidly upregulated in ischemic brain tissue

287   by microglia and macrophages (Clausen et al., 2016; Yli-Karjanmaa et al., 2019). The synergistic

288   stimulation of IL-17 receptor positive target cells, such as astrocytes, by IL-17A and IL-1β and/or

289   TNF-α induces an amplification of pro-inflammatory factors in the ischemic brain (Gelderblom et

290   al., 2012). Once the acute injury has subsided, the decrease in synergistic pro-inflammatory

291   cytokines might result in more neuro-regenerative effects of IL-17A (Lin et al., 2016). For this

292   reason, a therapeutic interference with anti-IL17A antibodies should be of short duration and

293   limited to the acute stage of stroke.

294   In the ischemic brain of the mouse, we could show that IL-17A is produced by vγ6[+] γδ T cells

295   (Arunachalam et al., 2017). These data and our current study have the drawback that they stem

296   from studies in young male mice, which do not reflect the human stroke population. Human

297   stroke patients are older and typically suffer from comorbidities such as atherosclerosis,

298   hypertension, and diabetes. In addition, the cellular source of IL-17A in humans is less well

299   understood. In human autoimmunity, IL-17A producing immune cells encompass CD8^{+} T cells,

300   Th17 cells, NK cells, NKT cell, neutrophils, and mast cells (reviewed by (Lubberts, 2015)).

301   However, the IL-17A pathway is highly conserved between mammals and downstream pathways

302   such as chemotaxis are comparable (Veldhoen, 2017). We could show that IL-17A producing

303   cells and neutrophils infiltrate ischemic human brains at early stages (Gelderblom et al., 2012).

304   These facts provide clear evidence that the IL-17A axis contributes to human stroke.

18

305   Another strong modulator of immune responses is the microbiome (Kamada, Seo, Chen, &

306   Nunez, 2013). The microbiome has the potential to exert both pro- and anti-inflammatory

307   responses and is intimately linked to the proper function of our immune system (Kamada et al.,

308   2013; Round & Mazmanian, 2009). This influence is also observed on γδ T cells. The

309   microbiome impacts their proliferation, activation as well as their IL-17A secretion (Singh et al.,

310   2016; Zhang et al., 2019). Particularly, segmented filamentous bacteria (SFB) shape the IL-17A

311   polarization. Accordingly Ivanov et al. could show that there is a shift towards increased Th17

312   cells in the gut of mice colonized by SFB (Ivanov et al., 2009). In stroke, recolonizing germ-free

313   mice with dysbiotic microbiota increases lesion volume through a proinflammatory T cell

314   polarization (Singh et al., 2016). Even further, Benakis et al. demonstrated that the gut

315   microbiome influences the presence of IL-17A and the outcome following stroke (Benakis et al.,

316   2016). Taken together, there is clear evidence that the microbiome has a substantial impact on the

317   IL-17A response and should be considered in any study dealing with IL-17A neutralization or

318   even any immune modulation. In our study, we can demonstrate substantial heterogeneity within

319   the microbiome among the four participating centers. This reflects the heterogeneity in human

320   cohorts (Hall, Tolonen, & Xavier, 2017) and does not eliminate the effect of anti-IL-17A

321   treatment. However, when we analyzed the presence of SFB, we found that the center with the

322   highest SFB level showed no effect of the IL-17A neutralization. This finding suggests that

323   higher levels of IL-17A might diminish the effectiveness of our IL-17A antibody, at least of the

324   applied dosage. Thus, an adaptation of the anti-IL-17A dosage might be required in individuals

325   with constitutively elevated IL-17A levels.

326   The last 20 years have seen two milestones in stroke treatment: i.v. thrombolysis (National

327   Institute of Neurological & Stroke rt, 1995) and more recently the mechanical recanalization

328   (Berkhemer et al., 2015). While the reconstitution of the blood flow has certainly been helpful in

19

329 a subgroup of stroke patients, still only a minority benefits from the treatment. Therefore, it is

330 crucial that new targets are being developed. We believe that IL-17A could be such a promising

331 target. Our pRCT trial offers the best possible preclinical data basis to design a trial in humans

332 with strokes due to large vessel occlusions. In this scenario anti-IL-17A treatment could follow

333 endovascular thrombectomy.

334

335 **Material and methods**

336 Study design:

337 The study was performed between 2017 (initiation) and 2018 (unblinding) in an international

338 consortium consisting of four test centers. The infarct size was the primary endpoint. Secondary

339 endpoints were mortality, neurological outcome and neutrophil infiltration. The Hamburg study

340 center (M.G.) initiated the trial, coordinated the study design and performed central data analysis.

341 Hamburg (M.G.), New York (J.A.), Odense (B.C.) and Münster (J.M.) performed the tMCAO

342 experiments. Sample size per stroke model was determined a priori by performing a power

343 analysis (Power=0.95, G-Power). The group sizes were based on published data.

344

345 Mice:

346 C57Bl/6 mice were provided by different suppliers (Münster and Hamburg: Charles River,

347 Odense: Taconic, New York: The Jackson Lab) and kept in the respective animal facility at least

348 two weeks before experiments started. We used male mice with an age of 11 to 13 weeks and a

349 bodyweight of 24 to 28 g. In total, 136 mice were randomized and treated. The animals were

350 housed under the local guidelines of each study center and assessed at least once a day.

351

352   Transient middle cerebral artery occlusion (tMCAO):

353   Temporary middle cerebral artery occlusion was achieved by using the intraluminal filament

354   method (Doccol: Filament # 602112PK10) as previously described for 45 min (Gelderblom et al.,

355   2009). All mice were monitored for heart rate, rectal body temperature, and cerebral blood flow

356   with the use of transcranial temporal laser Doppler scans. The cerebral blood flow in the area of

357   the MCA showed a reduction by 80%, which did not differ between groups (data not shown).

358   Heart rate, and rectal body temperature also showed no difference in our cohorts. After stroke

359   induction, every mouse was repeatedly scored on a scale from 0 to 5 (0, no deficit; 1, preferential

360   turning; 2, circling; 3, longitudinal rolling; 4, no movement; and 5, death) immediately after

361   reawakening and every day until killing. Mice were sacrificed three days after tMCAO and

362   perfused with phosphate-buffered saline (PBS) and paraformaldehyde (PFA) 4% afterward. Mice

363   that did not survive until day three were excluded for the further analysis of the primary outcome

364   parameter. Brains were kept in 4% PFA for 24h, stored in PBS, and sent to Hamburg for further

365   analysis.

366

367   Infarct volume assessment by Magnetic Resonance Imaging:

368   The measurements of the specimens from Odense, New York and Münster were performed on a

369   7 Tesla system (ClinScan, Bruker). The specimens from Hamburg were measured on a 9,4 Tesla

370   system (BioSpec, Bruker). For the MRI acquisition, brains were placed in 15 ml PBS filled

371   falcons. The imaging protocol comprised an apparent diffusion coefficient (ADC) and diffusion-

372   weighted images (DWI). Calculations of infarct volumes were performed on ADC images using

373   ImageJ (NIH). Infarct sizes were corrected for brain edema (Gerriets et al., 2004). The rating of

374   the infarct volumes was performed by two independent and blinded raters. The comparison of the

375   infarct sizes of the two investigators revealed a highly significant correlation (Supplemental

376   Figure 4). MRI scans and all analysis files were stored on a central database.

377

378   Immunohistochemistry:

379   Following MRI, the PFA fixed brains were embedded in paraffin. Coronal sections of 10 μm

380   thickness were collected every 400 μm. For the immunostaining of neutrophils, we performed

381   antigen retrieval in 10 mM citrate buffer (pH 6.0) and blocked with normal rabbit serum. Ly-6G

382   clone 1A8 (1/500, Biolegend) was incubated overnight at 4°C. Vectastain Elite ABC HRP kit

383   (Rabbit-anti-rat secondary AB, 1/200) was used for visualization of the secondary antibody. For

384   nuclear staining, Nuclear Fast Red (SigmaAldrich) was added for 5 minutes on RT. Images were

385   acquired on a digital slide scanner (Hamamatsu; Nano Zoomer). Manual cell counting was done

386   with the NDP viewer (Hamamatsu). Individual neutrophils on the entire slide were marked by

387   hand in order to avoid double counts. Assignment to either the cortical or striatal group was

388   assessed by colocalization to the respective anatomical structure. Total numbers of neutrophils

389   were calculated according to the following calculation: Total number of neutrophils =

390     $N(n_1+n_2+…n_i)$ x 40 (N = Sum of all counted neutrophils in the brain, n_i = Number of neutrophils

391   counted in each $slide_i$ and 40 = Number of slides of 10 μm thickness in the position 1…i). For

392   each brain, neutrophils were analyzed in 15 slides. Images of representative neutrophils in both

393   groups were taken with a transmission light microscope (Apotome, Zeiss) and a 63x plan-

394   apochromatic oil DIC objective. For analysis of autoptic human brain tissue, cases were selected

395   from the files of the Institute of Neuropathology at the University Medical Center Hamburg-

396   Eppendorf. Brain specimens had been fixed in 4% buffered formalin for at least two weeks

397   before paraffin-embedding. Brain sections (3 m thick) were stained according to standard

398   haematoxylin and eosin stain procedures.

399

400

401   Collection of feces:

402   We collected feces of 10 mice in each center for the analysis of the gut microbiome. All mice

403   housed for at least two weeks in the animal facility of the respective centers in order to adapt to

404   local microbiota. The specimens were collected early in the morning directly from each mouse in

405   order to avoid the loss of anaerobic bacteria. Immediately after collection, the feces were

406   homogenized in 96% ethanol to stop DNA degradation.

407

408   Nucleic Acid Extraction:

409   Nucleic acid (DNA and RNA) was extracted from 200 µl sample volume using an automated

410   extraction system, Qiasymphony (Qiagen, Hilden), according to the manufacturer's instructions.

411

412   16S rRNA amplicon library preparation, MiSeq sequencing, and bioinformatic analysis:

413   V3–V4 region 16S rRNA amplicon sequencing was performed as recently published (Lamprecht

414   et al., 2019). The following primers containing the Illumina adapter consensus sequence were

415   used: F: 5'-

416   TCGTCGGCAGCGTCAGATGTGTATAAGAGACAGCCTACGGGNGGCWGCAG-3 and R:

417   5-GTCTCGTGGGCTCGGAGATGTGTATAAGAGACAGGACTACHVGGGTATCTAATCC-

418   3. Samples were multiplexed using the Illumina Nextera XT Index Kit and sequenced by 500 PE

419   sequencing on the MiSeq platform. FastQC (Babraham Bioinformatics, Babraham Institute, UK)

420   was used to determine the average quality scores of each sample before and after paired reads.

421   The paired ends in each sample were joined, and all sequences less than 250 bp and/or with a

422   Phred score <33 were discarded. Quality filtering was applied using QIIME 53 (at Phred $\geq$ Q20).

423   We performed operational taxonomic unit (OTU) clustering and alpha- and beta-diversity

424   analysis using QIIME 2 (Bolyen et al., 2019). A chimera filter was applied using USEARCH 8.1.

425   All sequences were clustered based on 97% similarity to reference sequences. The reads that did

426   not meet the 97% similarity criteria were clustered de novo. Taxonomy levels of representative

427   sequences in the OTU table were assigned at 95% similarity based on the SILVA database. We

428   calculated alpha diversity based on the total amount of OTUs. Analysis of beta diversity statistics

429   (analysis of similarities, ANOSIM) was performed to determine if differences between the

430   distributions of microbiota profiles were significant.

431

432   Quantitative PCR analysis of Segmented Filamentous Bacteria (SFB):

433   RT-PCR was performed on 7 ng of purified fecal DNA in three technical replicates. PCR was

434   performed with Power SYBR Green PCR Master Mix (Thermofischer) on a Lightcycler 96

435   (Roche) with the following primers: SFB 736F: GACGCTGAGGCATGAGAGCAT, SFB 844R:

436   GACGGCACGRATTGTTATTCA, and universal bacterial r16S gene primers 16S-V2-101F:

437   AGYGGCGIACGGGTGAGTAA and 16S-V2-361R: CYIACTGCTGCCTCCCGTAG. Ct

438   values of SFB amplicons were normalized to r16S gene Ct values by the $\Delta\Delta$Ct method and data

439   are expressed as fold change over SFB levels in mice from Odense as reference group. Analysis

440   was performed with Excel (Microsoft) and GraphPad Prism.

441

24

442 Flow Cytometric analyzes:

443 Fluorescence-activated cell sorting (FACS) measurements were performed with an LSR Fortessa

444 (BD Biosciences). Data analysis was done with FlowJo (BD Biosciences). After PBS perfusion,

445 the removed brains were cut into 1 mm thick slices, and the cortex was dissected from the

446 striatum under a microscope. Only ipsilesional hemispheres were taken, digested for 30 min at

447 37°C (1 mg/ml collagenase, 0.1 mg/ml DNAse I in DMEM), and pressed through a 40 µm cell

448 strainer. Cells were incubated with standard erythrocyte lysis buffer on ice and separated from

449 myelin and debris by Percoll gradient (GE Healthcare) centrifugation. All antibodies were used

450 with a dilution of 1/100. Incubation was performed for 30 minutes at 4°C. For cell counting, BD

451 Trucount (BD Biosciences) tubes were taken. The following antibodies were used: Biolegend:

452 TCR γ/δ (Clone GL3), CD11b (M1/70), CD3 (17A2), B220 (RA3-6B2), F4/80 (BM8), CD8 (53-

453 6.7), NK1.1 (PK136), CD4 (RM4-59), eBioscience: MHCII (M5/114.15.2), CD11c (N418),

454 CD45 (30-F11), BD Bioscience: Ly6G (1A8).

455

456 Statistical Analysis:

457 We computed a generalized linear mixed model analysis (SPSS, IBM, © 2019) to test for

458 treatment effects on the infarct volume. This model allowed us to account for two raters as

459 random effects. Fixed effects were set as treatment and center in order to compute pairwise

460 contrasts between the treatment groups for each center. Normal distribution was checked

461 beforehand by histogram analysis. For the pairwise comparisons, p-values were adjusted with

462 Šidák`s correction in order to account for multiple testing. Each specimen was divided into one of

463 the two subgroups (with- and without cortical infarction) by two independent raters. Within each

464 subgroup, we conducted the same analysis as we did in the main group. Pearson's r was

465 calculated for interrater reliability. Mortality was analyzed with a log-rank test. Neuroscores were

466 analyzed with a Mann-Whitney test for non-parametric data and bodyweight was analyzed using

467 a mixed model analysis to account for missing values with time points and treatments as fixed

468 effects. Šidák`s test was assessed to test for pairwise contrasts of the two treatment groups on

469 each time point. Flow cytometric data on neutrophil infiltration was tested using a two-sided

470 student's t-test for dependent samples. Neutrophil counts from immunohistochemical studies

471 were analyzed with a multivariate analysis of variances with repeated measurements of variances

472 with compartments and treatments as independent variables. Šidák`s test was assessed to check

473 for pairwise contrasts of the two treatments in the two compartments. Differences in the OTUs

474 were assessed with t-tests for independent samples (QIIME 2). An analysis of similarities was

475 performed to test for significance in the beta-diversity (QIIME 2). RT-qPCR data were analyzed

476 with student's t-tests for independent samples. In all tests, the alpha level was set on 0.05. If not

477 stated otherwise GraphPad Prism 8 was used for the analysis.

478

479 **Appendix**

480 Study approval:

481 We conducted all experiments according to the Guide for the Care and Use of Laboratory

482 Animals published by the US National Institutes of Health (publication No. 83–123, revised

483 1996) and performed all procedures in accordance with the ARRIVE guidelines (Animal

484 Research: Reporting of In Vivo Experiments; http:// www.nc3rs.org/ARRIVE). All animal

485 experiments were approved by the respective local animal care committees.

486 Conflict of interest statement:

26

487   The authors declare no competing financial interests. No study sponsors had any influence on the

488   study design; in the collection, analysis, and interpretation of data; in the writing of the report;

489   and in the decision to submit the paper for publication.

490

491   Author contributions:

492   M.G. initiated this trial; M.G., T.M., J.M., J.A., B.H.C., T.V.A., G.T., and C.G. designed the

493   study protocol, supervised the study, reviewed, and verified original data sets. S.K. performed the

494   central analysis of infarct sizes. S.K., J.K.S., C.J., L.G.B., P.L., C.B., C.F., J.S. performed

495   experiments. S.K. and H.P. performed central statistical analysis. M.G., S.K., T.M., J.M., B.H.C.,

496   J.A., G.T., and C.G. wrote the manuscript.

497

498   Acknowledgments:

507

508   **References**

509   Alves de Lima, K., Rustenhoven, J., Da Mesquita, S., Wall, M., Salvador, A. F., Smirnov, I.,
510   Martelossi Cebinelli, G., Mamuladze, T., Baker, W., Papadopoulos, Z., Lopes, M. B., Cao,
511   W. S., Xie, X. S., Herz, J., & Kipnis, J. (2020). Meningeal gammadelta T cells regulate
512   anxiety-like behavior via IL-17a signaling in neurons. *Nat Immunol, 21*(11), 1421-1429.
513   doi:10.1038/s41590-020-0776-4
514   Arunachalam, P., Ludewig, P., Melich, P., Arumugam, T. V., Gerloff, C., Prinz, I., Magnus, T., &
515   Gelderblom, M. (2017). CCR6 (CC Chemokine Receptor 6) Is Essential for the Migration of
516   Detrimental Natural Interleukin-17-Producing gammadelta T Cells in Stroke. *Stroke,*
517   *48*(7), 1957-1965. doi:10.1161/STROKEAHA.117.016753
518   Baker, M. (2016). 1,500 scientists lift the lid on reproducibility. *Nature, 533*(7604), 452-454.
519   doi:10.1038/533452a
520   Benakis, C., Brea, D., Caballero, S., Faraco, G., Moore, J., Murphy, M., Sita, G., Racchumi, G.,
521   Ling, L., Pamer, E. G., Iadecola, C., & Anrather, J. (2016). Commensal microbiota affects
522   ischemic stroke outcome by regulating intestinal gammadelta T cells. *Nat Med*.
523   doi:10.1038/nm.4068
524   Berkhemer, O. A., Fransen, P. S., Beumer, D., van den Berg, L. A., Lingsma, H. F., Yoo, A. J.,
525   Schonewille, W. J., Vos, J. A., Nederkoorn, P. J., Wermer, M. J., van Walderveen, M. A.,
526   Staals, J., Hofmeijer, J., van Oostayen, J. A., Lycklama a Nijeholt, G. J., Boiten, J., Brouwer,
527   P. A., Emmer, B. J., de Bruijn, S. F., van Dijk, L. C., Kappelle, L. J., Lo, R. H., van Dijk, E. J.,
528   de Vries, J., de Kort, P. L., van Rooij, W. J., van den Berg, J. S., van Hasselt, B. A., Aerden,
529   L. A., Dallinga, R. J., Visser, M. C., Bot, J. C., Vroomen, P. C., Eshghi, O., Schreuder, T. H.,
530   Heijboer, R. J., Keizer, K., Tielbeek, A. V., den Hertog, H. M., Gerrits, D. G., van den Berg-
531   Vos, R. M., Karas, G. B., Steyerberg, E. W., Flach, H. Z., Marquering, H. A., Sprengers, M.
532   E., Jenniskens, S. F., Beenen, L. F., van den Berg, R., Koudstaal, P. J., van Zwam, W. H.,
533   Roos, Y. B., van der Lugt, A., van Oostenbrugge, R. J., Majoie, C. B., Dippel, D. W., &
534   Investigators, M. C. (2015). A randomized trial of intraarterial treatment for acute
535   ischemic stroke. *N Engl J Med, 372*(1), 11-20. doi:10.1056/NEJMoa1411587
536   Bolyen, E., Rideout, J. R., Dillon, M. R., Bokulich, N. A., Abnet, C. C., Al-Ghalith, G. A., Alexander,
537   H., Alm, E. J., Arumugam, M., Asnicar, F., Bai, Y., Bisanz, J. E., Bittinger, K., Brejnrod, A.,
538   Brislawn, C. J., Brown, C. T., Callahan, B. J., Caraballo-Rodriguez, A. M., Chase, J., Cope, E.
539   K., Da Silva, R., Diener, C., Dorrestein, P. C., Douglas, G. M., Durall, D. M., Duvallet, C.,
540   Edwardson, C. F., Ernst, M., Estaki, M., Fouquier, J., Gauglitz, J. M., Gibbons, S. M.,
541   Gibson, D. L., Gonzalez, A., Gorlick, K., Guo, J., Hillmann, B., Holmes, S., Holste, H.,
542   Huttenhower, C., Huttley, G. A., Janssen, S., Jarmusch, A. K., Jiang, L., Kaehler, B. D.,
543   Kang, K. B., Keefe, C. R., Keim, P., Kelley, S. T., Knights, D., Koester, I., Kosciolek, T., Kreps,
544   J., Langille, M. G. I., Lee, J., Ley, R., Liu, Y. X., Loftfield, E., Lozupone, C., Maher, M.,
545   Marotz, C., Martin, B. D., McDonald, D., McIver, L. J., Melnik, A. V., Metcalf, J. L., Morgan,
546   S. C., Morton, J. T., Naimey, A. T., Navas-Molina, J. A., Nothias, L. F., Orchanian, S. B.,
547   Pearson, T., Peoples, S. L., Petras, D., Preuss, M. L., Pruesse, E., Rasmussen, L. B., Rivers,
548   A., Robeson, M. S., 2nd, Rosenthal, P., Segata, N., Shaffer, M., Shiffer, A., Sinha, R., Song,
549   S. J., Spear, J. R., Swafford, A. D., Thompson, L. R., Torres, P. J., Trinh, P., Tripathi, A.,
550   Turnbaugh, P. J., Ul-Hasan, S., van der Hooft, J. J. J., Vargas, F., Vazquez-Baeza, Y.,
551   Vogtmann, E., von Hippel, M., Walters, W., Wan, Y., Wang, M., Warren, J., Weber, K. C.,

552   Williamson, C. H. D., Willis, A. D., Xu, Z. Z., Zaneveld, J. R., Zhang, Y., Zhu, Q., Knight, R., &
553   Caporaso, J. G. (2019). Author Correction: Reproducible, interactive, scalable and
554   extensible microbiome data science using QIIME 2. *Nat Biotechnol, 37*(9), 1091.
555   doi:10.1038/s41587-019-0252-6
556   Chamorro, A., Dirnagl, U., Urra, X., & Planas, A. M. (2016). Neuroprotection in acute stroke:
557   targeting excitotoxicity, oxidative and nitrosative stress, and inflammation. *Lancet*
558   *Neurol, 15*(8), 869-881. doi:10.1016/S1474-4422(16)00114-9
559   Clausen, B. H., Lambertsen, K. L., Dagnaes-Hansen, F., Babcock, A. A., von Linstow, C. U.,
560   Meldgaard, M., Kristensen, B. W., Deierborg, T., & Finsen, B. (2016). Cell therapy
561   centered on IL-1Ra is neuroprotective in experimental stroke. *Acta Neuropathol, 131*(5),
562   775-791. doi:10.1007/s00401-016-1541-5
563   Collaborators, G. B. D. S. (2019). Global, regional, and national burden of stroke, 1990-2016: a
564   systematic analysis for the Global Burden of Disease Study 2016. *Lancet Neurol, 18*(5),
565   439-458. doi:10.1016/S1474-4422(19)30034-1
566   Cua, D. J., & Tato, C. M. (2010). Innate IL-17-producing cells: the sentinels of the immune
567   system. *Nat Rev Immunol, 10*(7), 479-489. doi:10.1038/nri2800
568   Dai, Q., Han, S., Liu, T., Zheng, J., Liu, C., Li, J., & Li, S. (2020). IL-17A Neutralization Improves the
569   Neurological Outcome of Mice With Ischemic Stroke and Inhibits Caspase-12-Dependent
570   Apoptosis. *Front Aging Neurosci, 12*, 274. doi:10.3389/fnagi.2020.00274
571   Dirnagl, U., Hakim, A., Macleod, M., Fisher, M., Howells, D., Alan, S. M., Steinberg, G., Planas, A.,
572   Boltze, J., Savitz, S., Iadecola, C., & Meairs, S. (2013). A concerted appeal for
573   international cooperation in preclinical stroke research. *Stroke, 44*(6), 1754-1760.
574   doi:10.1161/STROKEAHA.113.000734
575   Elkind, M. S. V., Veltkamp, R., Montaner, J., Johnston, S. C., Singhal, A. B., Becker, K., Lansberg,
576   M. G., Tang, W., Kasliwal, R., & Elkins, J. (2020). Natalizumab in acute ischemic stroke
577   (ACTION II): A randomized, placebo-controlled trial. *Neurology, 95*(8), e1091-e1104.
578   doi:10.1212/WNL.0000000000010038
579   Elkins, J., Veltkamp, R., Montaner, J., Johnston, S. C., Singhal, A. B., Becker, K., Lansberg, M. G.,
580   Tang, W., Chang, I., Muralidharan, K., Gheuens, S., Mehta, L., & Elkind, M. S. V. (2017).
581   Safety and efficacy of natalizumab in patients with acute ischaemic stroke (ACTION): a
582   randomised, placebo-controlled, double-blind phase 2 trial. *Lancet Neurol, 16*(3), 217-
583   226. doi:10.1016/S1474-4422(16)30357-X
584   Ganesan, V., Ng, V., Chong, W. K., Kirkham, F. J., & Connelly, A. (1999). Lesion volume, lesion
585   location, and outcome after middle cerebral artery territory stroke. *Arch Dis Child, 81*(4),
586   295-300. doi:10.1136/adc.81.4.295
587   Gelderblom, M., Leypoldt, F., Steinbach, K., Behrens, D., Choe, C. U., Siler, D. A., Arumugam, T.
588   V., Orthey, E., Gerloff, C., Tolosa, E., & Magnus, T. (2009). Temporal and spatial dynamics
589   of cerebral immune cell accumulation in stroke. *Stroke, 40*(5), 1849-1857.
590   doi:10.1161/STROKEAHA.108.534503
591   Gelderblom, M., Weymar, A., Bernreuther, C., Velden, J., Arunachalam, P., Steinbach, K., Orthey,
592   E., Arumugam, T. V., Leypoldt, F., Simova, O., Thom, V., Friese, M. A., Prinz, I., Holscher,
593   C., Glatzel, M., Korn, T., Gerloff, C., Tolosa, E., & Magnus, T. (2012). Neutralization of the
594   IL-17 axis diminishes neutrophil invasion and protects from ischemic stroke. *Blood,*
595   *120*(18), 3793-3802. doi:10.1182/blood-2012-02-412726

596 Gerriets, T., Stolz, E., Walberer, M., Muller, C., Kluge, A., Bachmann, A., Fisher, M., Kaps, M., &
597   Bachmann, G. (2004). Noninvasive quantification of brain edema and the space-
598   occupying effect in rat stroke models using magnetic resonance imaging. *Stroke, 35*(2),
599   566-571. doi:10.1161/01.STR.0000113692.38574.57

600 Hall, A. B., Tolonen, A. C., & Xavier, R. J. (2017). Human genetic variation and the gut
601   microbiome in disease. *Nat Rev Genet, 18*(11), 690-699. doi:10.1038/nrg.2017.63

602 Ivanov, II, Atarashi, K., Manel, N., Brodie, E. L., Shima, T., Karaoz, U., Wei, D., Goldfarb, K. C.,
603   Santee, C. A., Lynch, S. V., Tanoue, T., Imaoka, A., Itoh, K., Takeda, K., Umesaki, Y.,
604   Honda, K., & Littman, D. R. (2009). Induction of intestinal Th17 cells by segmented
605   filamentous bacteria. *Cell, 139*(3), 485-498. doi:10.1016/j.cell.2009.09.033

606 Kamada, N., Seo, S. U., Chen, G. Y., & Nunez, G. (2013). Role of the gut microbiota in immunity
607   and inflammatory disease. *Nat Rev Immunol, 13*(5), 321-335. doi:10.1038/nri3430

608 Lamprecht, P., Fischer, N., Huang, J., Burkhardt, L., Lutgehetmann, M., Arndt, F., Rolfs, I.,
609   Kerstein, A., Iking-Konert, C., & Laudien, M. (2019). Changes in the composition of the
610   upper respiratory tract microbial community in granulomatosis with polyangiitis. *J
611   Autoimmun, 97*, 29-39. doi:10.1016/j.jaut.2018.10.005

612 Landis, S. C., Amara, S. G., Asadullah, K., Austin, C. P., Blumenstein, R., Bradley, E. W., Crystal, R.
613   G., Darnell, R. B., Ferrante, R. J., Fillit, H., Finkelstein, R., Fisher, M., Gendelman, H. E.,
614   Golub, R. M., Goudreau, J. L., Gross, R. A., Gubitz, A. K., Hesterlee, S. E., Howells, D. W.,
615   Huguenard, J., Kelner, K., Koroshetz, W., Krainc, D., Lazic, S. E., Levine, M. S., Macleod,
616   M. R., McCall, J. M., Moxley, R. T., 3rd, Narasimhan, K., Noble, L. J., Perrin, S., Porter, J.
617   D., Steward, O., Unger, E., Utz, U., & Silberberg, S. D. (2012). A call for transparent
618   reporting to optimize the predictive value of preclinical research. *Nature, 490*(7419),
619   187-191. doi:10.1038/nature11556

620 Lee, J., d'Aigle, J., Atadja, L., Quaicoe, V., Honarpisheh, P., Ganesh, B. P., Hassan, A., Graf, J.,
621   Petrosino, J., Putluri, N., Zhu, L., Durgan, D. J., Bryan, R. M., Jr., McCullough, L. D., &
622   Venna, V. R. (2020). Gut Microbiota-Derived Short-Chain Fatty Acids Promote Poststroke
623   Recovery in Aged Mice. *Circ Res, 127*(4), 453-465. doi:10.1161/CIRCRESAHA.119.316448

624 Lin, Y., Zhang, J. C., Yao, C. Y., Wu, Y., Abdelgawad, A. F., Yao, S. L., & Yuan, S. Y. (2016). Critical
625   role of astrocytic interleukin-17 A in post-stroke survival and neuronal differentiation of
626   neural precursor cells in adult mice. *Cell Death Dis, 7*(6), e2273.
627   doi:10.1038/cddis.2015.284

628 Lipsanen, A., & Jolkkonen, J. (2011). Experimental approaches to study functional recovery
629   following cerebral ischemia. *Cell Mol Life Sci, 68*(18), 3007-3017. doi:10.1007/s00018-
630   011-0733-3

631 Llovera, G., Hofmann, K., Roth, S., Salas-Perdomo, A., Ferrer-Ferrer, M., Perego, C., Zanier, E. R.,
632   Mamrak, U., Rex, A., Party, H., Agin, V., Fauchon, C., Orset, C., Haelewyn, B., De Simoni,
633   M. G., Dirnagl, U., Grittner, U., Planas, A. M., Plesnila, N., Vivien, D., & Liesz, A. (2015).
634   Results of a preclinical randomized controlled multicenter trial (pRCT): Anti-CD49d
635   treatment for acute brain ischemia. *Sci Transl Med, 7*(299), 299ra121.
636   doi:10.1126/scitranslmed.aaa9853

637 Lovblad, K. O., Baird, A. E., Schlaug, G., Benfield, A., Siewert, B., Voetsch, B., Connor, A.,
638   Burzynski, C., Edelman, R. R., & Warach, S. (1997). Ischemic lesion volumes in acute
639   stroke by diffusion-weighted magnetic resonance imaging correlate with clinical
640   outcome. *Ann Neurol, 42*(2), 164-170. doi:10.1002/ana.410420206

641   Lubberts, E. (2015). The IL-23-IL-17 axis in inflammatory arthritis. *Nat Rev Rheumatol, 11*(7),
642   415-429. doi:10.1038/nrrheum.2015.53
643   McGeachy, M. J., Cua, D. J., & Gaffen, S. L. (2019). The IL-17 Family of Cytokines in Health and
644   Disease. *Immunity, 50*(4), 892-906. doi:10.1016/j.immuni.2019.03.021
645   National Institute of Neurological, D., & Stroke rt, P. A. S. S. G. (1995). Tissue plasminogen
646   activator for acute ischemic stroke. *N Engl J Med, 333*(24), 1581-1587.
647   doi:10.1056/NEJM199512143332401
648   O'Collins, V. E., Macleod, M. R., Donnan, G. A., Horky, L. L., van der Worp, B. H., & Howells, D. W.
649   (2006). 1,026 experimental treatments in acute stroke. *Ann Neurol, 59*(3), 467-477.
650   doi:10.1002/ana.20741
651   Percie du Sert, N., Ahluwalia, A., Alam, S., Avey, M. T., Baker, M., Browne, W. J., Clark, A., Cuthill,
652   I. C., Dirnagl, U., Emerson, M., Garner, P., Holgate, S. T., Howells, D. W., Hurst, V., Karp,
653   N. A., Lazic, S. E., Lidster, K., MacCallum, C. J., Macleod, M., Pearl, E. J., Petersen, O. H.,
654   Rawle, F., Reynolds, P., Rooney, K., Sena, E. S., Silberberg, S. D., Steckler, T., & Wurbel, H.
655   (2020). Reporting animal research: Explanation and elaboration for the ARRIVE
656   guidelines 2.0. *PLoS Biol, 18*(7), e3000411. doi:10.1371/journal.pbio.3000411
657   Ribeiro, M., Brigas, H. C., Temido-Ferreira, M., Pousinha, P. A., Regen, T., Santa, C., Coelho, J. E.,
658   Marques-Morgado, I., Valente, C. A., Omenetti, S., Stockinger, B., Waisman, A., Manadas,
659   B., Lopes, L. V., Silva-Santos, B., & Ribot, J. C. (2019). Meningeal gammadelta T cell-
660   derived IL-17 controls synaptic plasticity and short-term memory. *Sci Immunol, 4*(40).
661   doi:10.1126/sciimmunol.aay5199
662   Round, J. L., & Mazmanian, S. K. (2009). The gut microbiota shapes intestinal immune responses
663   during health and disease. *Nat Rev Immunol, 9*(5), 313-323. doi:10.1038/nri2515
664   Ruddy, M. J., Wong, G. C., Liu, X. K., Yamamoto, H., Kasayama, S., Kirkwood, K. L., & Gaffen, S. L.
665   (2004). Functional cooperation between interleukin-17 and tumor necrosis factor-alpha
666   is mediated by CCAAT/enhancer-binding protein family members. *J Biol Chem, 279*(4),
667   2559-2567. doi:10.1074/jbc.M308809200
668   Schmidt-Pogoda, A., Bonberg, N., Koecke, M. H. M., Strecker, J. K., Wellmann, J., Bruckmann, N.
669   M., Beuker, C., Schabitz, W. R., Meuth, S. G., Wiendl, H., Minnerup, H., & Minnerup, J.
670   (2020). Why Most Acute Stroke Studies Are Positive in Animals but Not in Patients: A
671   Systematic Comparison of Preclinical, Early Phase, and Phase 3 Clinical Trials of
672   Neuroprotective Agents. *Ann Neurol, 87*(1), 40-51. doi:10.1002/ana.25643
673   Shichita, T., Sugiyama, Y., Ooboshi, H., Sugimori, H., Nakagawa, R., Takada, I., Iwaki, T., Okada,
674   Y., Iida, M., Cua, D. J., Iwakura, Y., & Yoshimura, A. (2009). Pivotal role of cerebral
675   interleukin-17-producing gammadeltaT cells in the delayed phase of ischemic brain
676   injury. *Nat Med, 15*(8), 946-950. doi:10.1038/nm.1999
677   Singh, V., Roth, S., Llovera, G., Sadler, R., Garzetti, D., Stecher, B., Dichgans, M., & Liesz, A.
678   (2016). Microbiota Dysbiosis Controls the Neuroinflammatory Response after Stroke. *J
679   Neurosci, 36*(28), 7428-7440. doi:10.1523/JNEUROSCI.1114-16.2016
680   Sommer, C. J. (2017). Ischemic stroke: experimental models and reality. *Acta Neuropathol,
681   133*(2), 245-261. doi:10.1007/s00401-017-1667-0
682   Veldhoen, M. (2017). Interleukin 17 is a chief orchestrator of immunity. *Nat Immunol, 18*(6),
683   612-621. doi:10.1038/ni.3742
684   Xia, G. H., You, C., Gao, X. X., Zeng, X. L., Zhu, J. J., Xu, K. Y., Tan, C. H., Xu, R. T., Wu, Q. H., Zhou,
685   H. W., He, Y., & Yin, J. (2019). Stroke Dysbiosis Index (SDI) in Gut Microbiome Are

686   Associated With Brain Injury and Prognosis of Stroke. *Front Neurol, 10*, 397.

687   doi:10.3389/fneur.2019.00397

688 Yli-Karjanmaa, M., Clausen, B. H., Degn, M., Novrup, H. G., Ellman, D. G., Toft-Jensen, P.,

689   Szymkowski, D. E., Stensballe, A., Meyer, M., Brambilla, R., & Lambertsen, K. L. (2019).

690   Topical Administration of a Soluble TNF Inhibitor Reduces Infarct Volume After Focal

691   Cerebral Ischemia in Mice. *Front Neurosci, 13*, 781. doi:10.3389/fnins.2019.00781

692 Zhang, H., Carnevale, G., Polese, B., Simard, M., Thurairajah, B., Khan, N., Gentile, M. E., Fontes,

693   G., Vinh, D. C., Pouliot, R., & King, I. L. (2019). CD109 Restrains Activation of Cutaneous

694   IL-17-Producing gammadelta T Cells by Commensal Microbiota. *Cell Rep, 29*(2), 391-405

695   e395. doi:10.1016/j.celrep.2019.09.003

696

697

698

699

700

701

702

703

704

705

706

707

708

709

710

711

712 **Supplemental Material**

713

714 Supplemental figure 1:

715

716 Study design, attached separately

717

Supplemental Figure 2

718
719
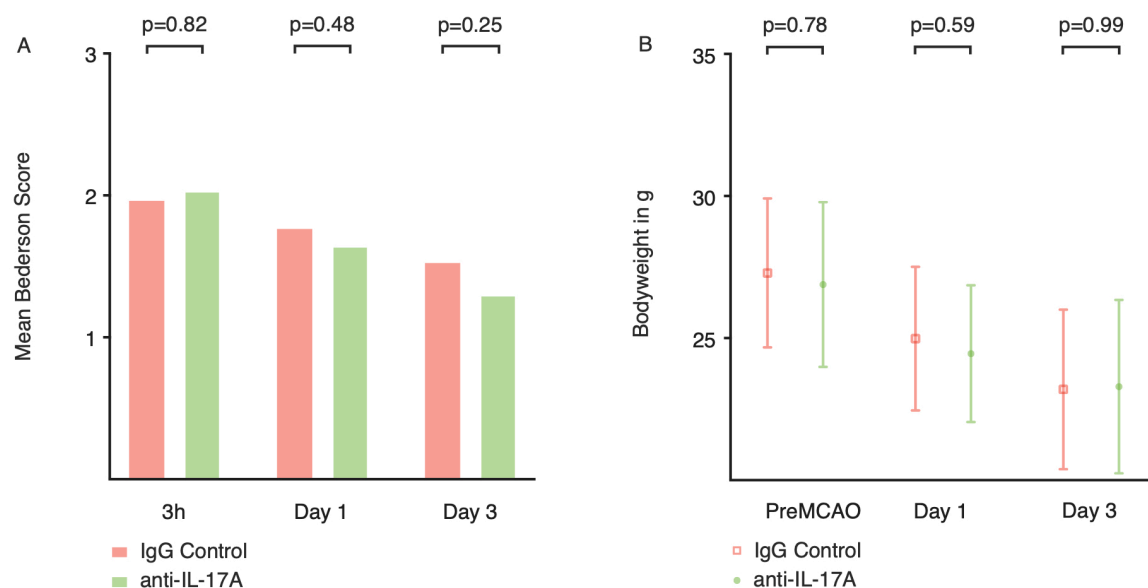
720 **Supplemental Figure 2. Bederson Neuroscore and bodyweight as secondary outcome**
721 **parameters.**

722 (A) Neurological scores at 3h and at days 1 and 3 of animals that were treated with 500 μg
723 isotype control or 500μg of anti-IL-17A. Significance was assessed by Mann-Whitney-U Test (3
724 hours: U=1878, p=0.82, n=62 in both groups, Day 1: U=1417, p=0.48, n= 59 in the anti IL-17A
725 group and n=52 in the IgG control group. Day 3: U=1341, p=0.25, n=60 in the anti IL-17A group
726 and n=51 in the IgG control group). (B) Bodyweight in g of mice of both treatment groups.
727 Statistical analysis was performed with a linear mixed model analysis and Šidák's multiple
728 comparison tests for pairwise comparisons (PreMCAO: $t_{(125.4)}$=0.84, p=0.78, n=128. Day 1:
729 $t_{(109.4)}$=1.14, p=0.59, n=114. Day 3: $t_{(106.3)}$=0.17, p=0.99, n=109).

730

33

Supplemental Figure 3

731
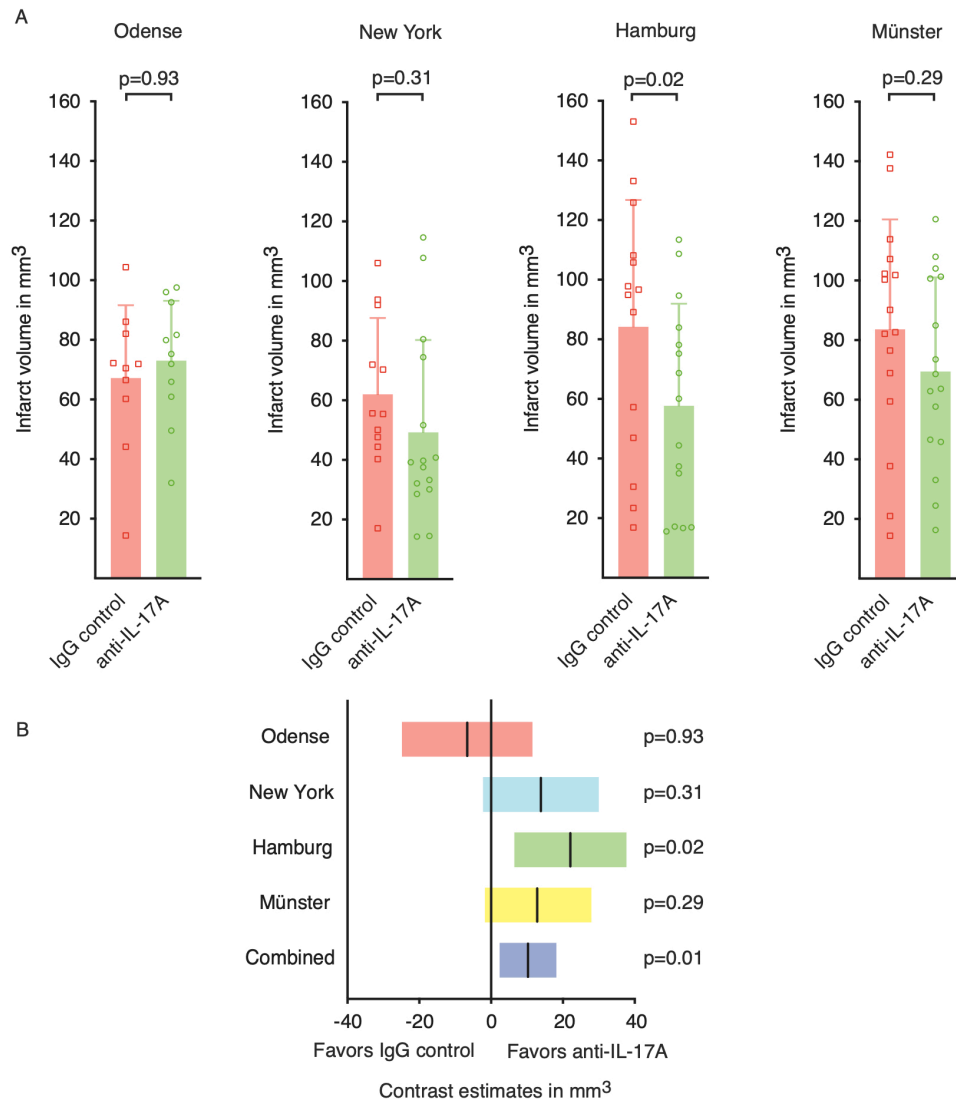
Supplemental Figure 3. Infarct size divided into individual centers.

(A) The infarct sizes of rater one in mm^3 for each individual center. Infarct volumes were
analyzed three days following tMCAO by MRI. Graphs show mean±SDs. Statistical significance
was assessed by linear-mixed model analysis with pairwise comparisons. (B) Pairwise
comparisons of infarct volumes for single centers. Post-hoc Šidák adjustments were made for the
alpha level. The estimated difference is shown in mm^3±95% CI (Odense: $F_{(1,209)}$=0.51, p=0.93,
n=21; New York: $F_{(1,209)}$=3.04, p=0.31, n=27; Hamburg: $F_{(1,209)}$=7.76, p=0.02, n=29; Münster:
$F_{(1,209)}$=2.88, p=0.29, n=32).

Supplemental Figure 4

740
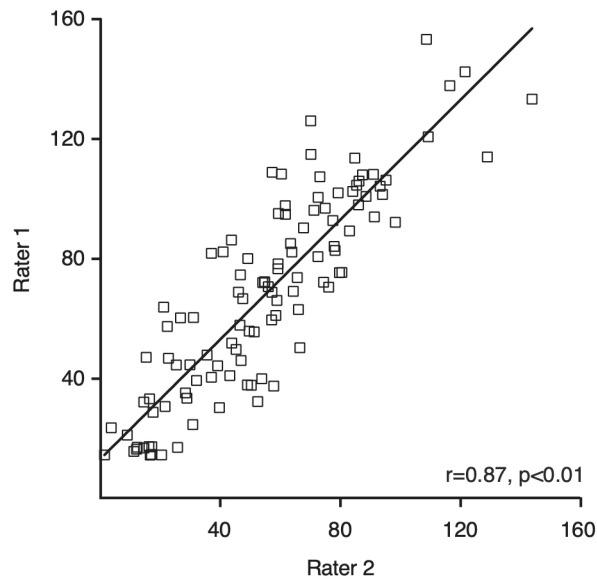
Supplemental Figure 4. Comparison of the volumetry of the raters.

Correlation of MRI based ratings of infarct volumes of rater one and two (Pearson r=0.87, CI = 0.82 – 0.91, p<0.001, n=109 pairs).